

Preparation and characterization of sulfamic acid pyridinium chloride-functionalized Fe₃O₄ nanoparticles as a novel magnetic catalyst for synthesis of novel *N*-coumarin-2-furanones

Sakineh Asghari^{1,2} · Majid Mohammadnia¹

Received: 25 May 2017 / Accepted: 10 July 2017 / Published online: 19 July 2017
© Springer Science+Business Media B.V. 2017

Abstract Sulfamic acid pyridinium chloride-functionalized Fe₃O₄ nanoparticles as a novel organic-inorganic hybrid heterogeneous catalyst was manufactured and characterized by FT-IR, XRD, TGA, SEM, TEM and VSM techniques. The catalytic activity of the nanomagnetic catalyst was investigated in the multicomponent reactions of arylaldehydes, 7-amino-4-methylcoumarin and dialkyl acetylenedicarboxylate that afford the novel *N*-coumarin-2-furanones. This green nanocatalytic procedure has good reversibility and provides clean production in a short reaction time.

Keywords Nanomagnetic catalyst · Arylaldehydes · 7-Amino-4-methylcoumarin · Dialkyl acetylenedicarboxylate · *N*-Coumarin-2-furanones

Introduction

Nanomaterials are of great interest in organic synthesis due to their extremely small size and large surface-to-volume ratio, which lead to both chemical and physical differences in their properties compared to bulk of the same chemical composition, such as mechanical, biological and satirical properties, higher catalytic activity, thermal and electrical conductivity, optical absorption and melting point [1–3]. Surface-functionalized iron oxide magnetic nanoparticles (MNPs) have been widely used in biotechnology and catalysis [4–8]. MNPs can easily be separated and recycled from the products by their response to an external magnetic field. Good

✉ Sakineh Asghari
s.asghari@umz.ac.ir

¹ Department of Organic Chemistry, Faculty of Chemistry, University of Mazandaran, Babolsar 47416-95447, Iran

² Nano and Biotechnology Research Group, University of Mazandaran, Babolsar, Iran

biocompatibility and biodegradability as well as basic magnetic characteristics could be designated for functional organic materials grafted to an MNP [9–12].

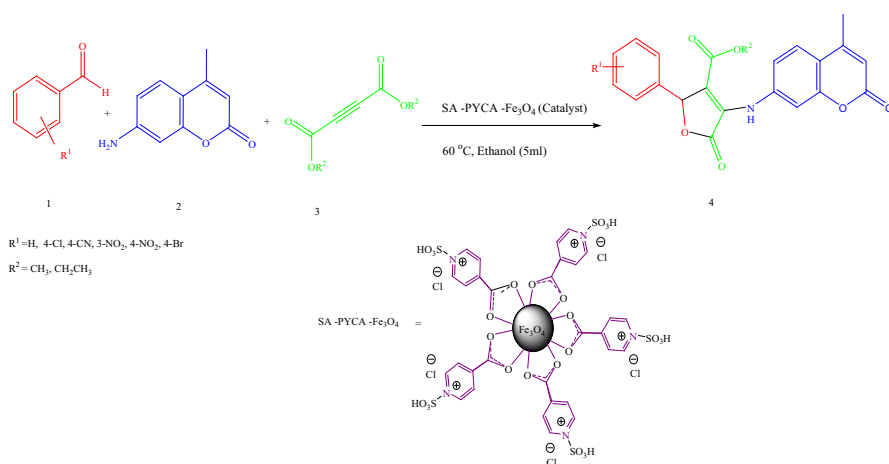
Multicomponent reactions (MCRs) belong to the most challenging areas of modern chemistry for several reasons such as reduction of the number of steps, time savings, material savings, higher yields than in comparable multistep reactions and fewer by-products [13–15]. Synthesis of medicine and complex molecules should be easy and efficient with minimal workup in this methodology [16, 17].

2-furanone derivatives are applicable synthetic modules in organic synthesis and are the main structural elements present in many pharmaceutical active products [18, 19]. Additionally, the coumarins are present in a variety of naturally occurring compounds that have antiallergic, antidiabetic, analgesic, anticoagulant, anticancer, antianaphylactia, antibacterial and fungicidal activities [20–24]. These results encouraged us to synthesize novel *N*-coumarin-2-furanones using MCRs. In continuation of our research on synthesis of heterocyclic compounds in the presence of nanomagnetic catalyst [25, 26], herein we wish to describe the preparation of novel *N*-coumarin-2-furanone derivatives **4** from reactions of various arylaldehydes **1**, 7-amino-4-methylcoumarin **2** and dialkyl acetylenedicarboxylate **3** in the presence of sulfamic acid pyridinium chloride-functionalized Fe_3O_4 nanoparticles (SA-PYCA- Fe_3O_4) as a novel green catalyst (Scheme 1).

Experimental

Chemicals and materials

Melting points were measured on an Electrothermal 9100 apparatus. The X-ray powder diffraction (XRD) of the catalyst was carried out on a Philips PW 1830

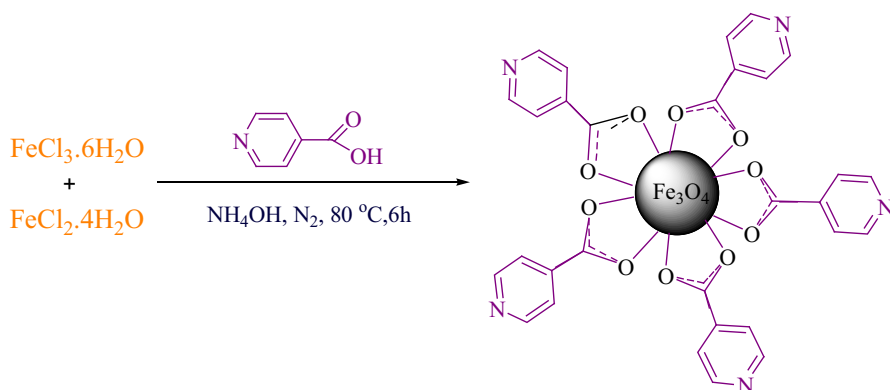


Scheme 1 Synthesis of novel *N*-coumarin-2-furanones **4** derivatives in the presences of SA-PYCA- Fe_3O_4 nanocatalyst

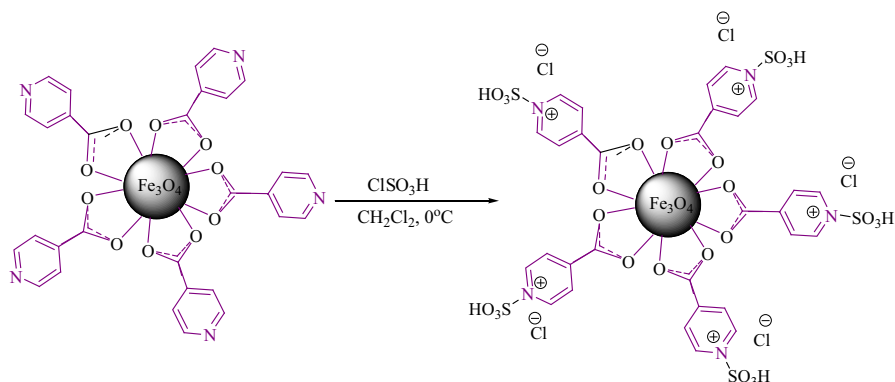
X-ray diffractometer with $\text{CuK}\alpha$ source ($\lambda = 1.5418 \text{ \AA}$) in a range of Bragg's angle ($10\text{--}80^\circ$) at room temperature. Scanning electron microscopy (SEM) analyses were conducted using a VEGA//TESCAN KYKY-EM 3200 microscope (acceleration voltage 26 kV). Transmission electron microscopy (TEM) experiments were conducted on a Philips EM 208 electron microscope. Thermogravimetric analysis (TGA) was recorded on a Stanton Red craft STA-780 (London, UK). Nuclear magnetic resonance (NMR) spectra were recorded with a Bruker DRX-400 AVANCE instrument (400.1 MHz for ^1H , 100.6 MHz for ^{13}C). The spectra were measured in DMSO-d_6 as solvent. Mass spectra were recorded on a Finnigan-Matt 8430 mass spectrometer operating at an ionization potential of 70 eV. Elemental analyses were performed using a Heracus CHN-O Rapid analyzer. IR spectra were recorded on an FT-IR Bruker vector 22 spectrophotometer. Magnetic measurements were performed using vibration sample magnetometer (VSM, MDK, and Model 7400) analysis.

Preparation of pyridine-4-carboxylic acid-functionalized Fe_3O_4 nanoparticles ($\text{Fe}_3\text{O}_4\text{-PYCA}$)

$\text{FeCl}_3 \cdot 6\text{H}_2\text{O}$ and $\text{FeCl}_2 \cdot 4\text{H}_2\text{O}$ (molar ratio 1:2) were added to 80 mL of deionized water and sonicated until the salts dissolved completely. Then, a predetermined amount of pyridine-4-carboxylic acid and ammonium hydroxide solution were added to the above mixture under N_2 atmosphere at room temperature until the pH was raised to 11. The color of the reaction solution turned black immediately, indicating the spontaneous formation of nanoparticles. This suspension was then refluxed at 100°C for a designed period of time and was then cooled to ambient room temperatures. After the complete reaction, the $\text{Fe}_3\text{O}_4\text{-PYCA}$ nanoparticles were separated by a magnetic field, washed with distilled water five times and then dried in an oven for 12 h (Scheme 2) [25].



Scheme 2 Preparation of $\text{Fe}_3\text{O}_4\text{-PYCA}$ nanoparticles



Scheme 3 Preparation of SA-PYCA-Fe₃O₄ nanoparticles

Preparation of novel sulfamic acid pyridinium chloride-functionalized Fe₃O₄ nanoparticles (SA-PYCA-Fe₃O₄)

The Fe₃O₄-PYCA (0.5 g) was dispersed in dry CH₂Cl₂ (10 mL) by ultrasonic bath for 30 min. Eventually, chlorosulfuric acid (0.7 mL) was added dropwise over a period of 25 min at room temperature. Hydrogen gas expelled from the reaction. Then, the prepared functionalized MNPs were separated by magnetic field and washed with dry CH₂Cl₂ four times to remove the unattached substrates (Scheme 3).

General procedure for the synthesis of novel N-coumarin-2-furanone derivatives by SA-PYCA-Fe₃O₄

To a mixture of arylaldehydes (1 mmol), 7-amino-4-methylcoumarin (1 mmol) and dialkyl acetylenedicarboxylate (1 mmol) in ethanol (5 mL) was added SA-PYCA-Fe₃O₄ (15 mg) as a nanocatalyst. The mixture was stirred at 60 °C for 2–3 h. When the reaction was completed (as monitored by thin layer chromatography (TLC)], the solvent was removed under reduced pressure. Then, the mixture was diluted with CH₂Cl₂ and the SA-PYCA-Fe₃O₄ nanoparticles were separated by a magnet field. The solution containing the product was evaporated to give the solid. The crude product was purified by washing with hot ethanol to give the desired product as a yellow powder.

Analytical data for all products:

Methyl 4-(4-methyl-2-oxo-2H-chromen-7-ylamino)-2,5-dihydro-5-oxo-2-phenylfuran-3-carboxylate (4a): Light yellow powder, melting point (m.p.): 220 °C; IR (KBr): ν_{\max} = 3340, 3067, 2955, 1717, 1657, 1615, 1434 cm⁻¹; ¹H NMR (400.13 MHz, DMSO): δ = 2.34 (s, 3H, CH₃), 3.60 (s, 3H, OCH₃), 6.21 (s, 1H, CH_{furan}), 6.28 (s, 1H, CH_{coumarin}), 7.17–7.26 (m, 3H, 3CH_{aromatic}), 7.33 (d, 2H, J = 7.2 Hz, 2CH_{aromatic}), 7.62–7.72 (m, 3H, 3CH_{aromatic}), 11.77 (s, 1H, N-H) ppm; ¹³C NMR (100.6 MHz, DMSO): δ = 18.4, 51.6, 60.7, 109.3, 112.9, 113.8, 116.9,

118.0, 126.2, 128.1, 128.5, 128.8, 136.7, 139.7, 152.7, 153.3, 153.5, 160.1, 162.8, 165 ppm. MS (EI, 70 eV) (%) 391 (M^+ , 100), 359 (25), 332 (16), 263 (29), 202 (50), 189 (46), 158 (13), 130(44); anal. calcd. for $C_{22}H_{17}NO_6$ (391.11): C, 67.51; H, 4.38; N, 3.58%; found: C, 67.78; H, 4.40; N, 3.55%.

Ethyl 4-(4-methyl-2-oxo-2H-chromen-7-ylamino)-2,5-dihydro-5-oxo-2-phenylfuran-3-carboxylate (4b): Light yellow powder, m.p.: 250–251 °C; IR (KBr): ν_{\max} = 3369, 3067, 2955, 2925, 1715, 1657, 1615, 1459 cm^{-1} ; 1H NMR (400.13 MHz, DMSO): δ = 1.59 (t, 3H, J = 8.4 Hz, CH_3), 2.35 (d, 3H, J = 0.8 Hz, CH_3), 3.99–4.10 (m, 2H, OCH_2), 6.21 (s, 1H, CH_{furan}), 6.28 (d, 1H, J = 1.2 Hz, CH_{coumarin}), 7.17 (t, 1H, J = 7.6 Hz, $1CH_{\text{aromatic}}$), 7.24 (t, 1H, J = 7.6 Hz, $1CH_{\text{aromatic}}$), 7.34 (d, 1H, J = 7.6 Hz, $1CH_{\text{aromatic}}$), 7.62–7.68 (m, 2H, $2CH_{\text{aromatic}}$), 7.72 (d, 1H, J = 2 Hz, $1CH_{\text{aromatic}}$), 11.71 (s, 1H, N–H) ppm; ^{13}C NMR (100.6 MHz, DMSO): δ = 14.4, 18.4, 60.3, 60.8, 109.3, 113.3, 113.8, 117.0, 118.0, 126.2, 128.2, 128.6, 128.8, 136.7, 139.8, 152.5, 153.4, 153.5, 160.2, 162.3, 165.0 ppm. MS (EI, 70 eV) (%) 405 (M^+ , 100), 359 (20), 332 (14), 203 (30), 158 (7), 130 (19); anal. calcd. for $C_{23}H_{19}NO_6$ (405.12): C, 68.14; H, 4.72; N, 3.46%; found: C, 68.11; H, 4.70; N, 3.41%.

Methyl 4-(4-methyl-2-oxo-2H-chromen-7-ylamino)-2-(4-cyanophenyl)-2,5-dihydro-5-oxofuran-3-carboxylate (4c): Light yellow powder, m.p.: 200–202 °C; IR (KBr): ν_{\max} = 3429, 3067, 2955, 2229, 1726, 1658, 1613, 1428 cm^{-1} ; 1H NMR (400.13 MHz, DMSO): δ = 2.35 (d, 3H, J = 0.8 Hz, CH_3), 3.60 (s, 3H, OCH_3), 6.30 (d, 1H, J = 0.8 Hz, CH_{coumarin}), 6.35 (s, 1H, CH_{furan}), 7.60–7.63 (m, 3H, $3CH_{\text{aromatic}}$), 7.67–7.73 (m, 4H, $4CH_{\text{aromatic}}$), 12.19 (s, 1H, N–H) ppm; ^{13}C NMR (100.6 MHz, DMSO): δ = 18.4, 51.8, 109.4, 11.4, 112.1, 114.0, 117.2, 117.9, 118.9, 126.4, 129.4, 132.8, 139.4, 142.7, 153.1, 153.3, 153.6, 160.1, 162.7, 164.8 ppm. MS (EI, 70 eV) (%) 416 (M^+ , 35), 384 (35), 358 (8), 288 (6), 214 (8), 202 (0.30), 155 (10); anal. calcd. for $C_{23}H_{16}N_2O_6$ (391.11): C, 66.34; H, 3.87; N, 6.73%; found: C, 66.31; H, 3.89; N, 6.74%.

Ethyl 4-(4-methyl-2-oxo-2H-chromen-7-ylamino)-2-(4-cyanophenyl)-2,5-dihydro-5-oxofuran-3-carboxylate (4d): Light yellow powder, m.p.: 255–256 °C; IR (KBr): ν_{\max} = 3421, 3061, 2925, 2231, 1724, 1686, 1648, 1613, 1425 cm^{-1} ; 1H NMR (400.13 MHz, DMSO): δ = 1.25 (t, 3H, J = 7.2 Hz, CH_3), 2.38 (d, 3H, J = 1.2 Hz, CH_3), 4.26 (q, 2H, J = 7.2 Hz, OCH_2), 5.85 (s, 1H, CH_{furan}), 6.26 (d, 1H, J = 1.2 Hz, CH_{coumarin}), 7.36 (d, 1H, J = 2.4 Hz, $1CH_{\text{aromatic}}$), 7.42 (d, 2H, J = 8.4 Hz, $2CH_{\text{aromatic}}$), 7.54 (d, 1H, J = 8.8 Hz, $1CH_{\text{aromatic}}$), 7.22 (d, 2H, J = 8.4 Hz, $2CH_{\text{aromatic}}$), 7.72 (dd, 1H, J = 8.8, 2.4 Hz, $1CH_{\text{aromatic}}$), 9.14 (s, 1H, N–H) ppm; ^{13}C NMR (100.6 MHz, DMSO): δ = 14.0, 18.5, 60.5, 61.9, 108.6, 112.8, 113.0, 114.6, 117.0, 117.5, 118.0, 125.5, 128.2, 132.8, 138.9, 140.2, 151.8, 153.9, 156.3, 160.4, 162.7, 164.5 ppm. MS (EI, 70 eV) (%) 430 (M^+ , 84), 384 (34), 357 (8), 228 (20), 202 (100), 155 (50); anal. calcd. for $C_{24}H_{18}N_2O_6$ (430.12): C, 66.97; H, 4.22; N, 6.51%; found: C, 66.96; H, 4.20; N, 6.53%.

Methyl 4-(4-methyl-2-oxo-2H-chromen-7-ylamino)-2,5-dihydro-2-(3-nitrophenyl)-5-oxofuran-3-carboxylate (4e): Light yellow powder, m.p.: 285–286 °C; IR

(KBr): ν_{\max} = 3263, 3092, 2953, 1730, 1659, 1613, 1528, 1435, 1384 cm^{-1} ; ^1H NMR (400.13 MHz, DMSO): δ = 2.50 (s, 3H, CH_3), 3.61 (s, 3H, OCH_3), 6.28 (s, 1H, $\text{CH}_{\text{coumarin}}$), 6.45 (s, 1H, CH_{furan}), 7.54 (t, 1H, J = 8 Hz, $1\text{CH}_{\text{aromatic}}$), 7.63–7.69 (m, 2H, $2\text{CH}_{\text{aromatic}}$), 7.78 (d, 1H, J = 1.6 Hz, $1\text{CH}_{\text{aromatic}}$), 7.22 (d, 1H, J = 8 Hz, $1\text{CH}_{\text{aromatic}}$), 8.08 (dd, 1H, J = 8, 1.6 Hz, $1\text{CH}_{\text{aromatic}}$), 8.35 (s, 1H, $1\text{CH}_{\text{aromatic}}$), 12.18 (s, 1H, N–H) ppm; ^{13}C NMR (100.6 MHz, DMSO): δ = 18.4, 51.8, 59.7, 109.5, 112.0, 114.0, 117.2, 118.0, 123.6, 123.7, 126.4, 130.5, 134.4, 139.3, 139.4, 148.1, 153.1, 153.2, 153.6, 160.1, 162.7, 164.8 ppm. MS (EI, 70 eV) (%) 436 (M^+ , 55), 404 (6), 348 (4), 308 (100), 261 (9), 201 (17), 175 (11); anal. calcd. for $\text{C}_{22}\text{H}_{16}\text{N}_2\text{O}_8$ (436.09): C, 60.55; H, 3.70; N, 6.42%; found: C, 60.52; H, 3.71; N, 6.40%.

Ethyl 4-(4-methyl-2-oxo-2H-chromen-7-ylamino)-2,5-dihydro-2-(3-nitrophenyl)-5-oxofuran-3-carboxylate (4f): Light yellow powder, m.p.: 270–271 °C; IR (KBr): ν_{\max} = 3434, 3089, 2986, 1728, 1651, 1613, 1528, 1439, 1357 cm^{-1} ; ^1H NMR (400.13 MHz, DMSO): δ = 1.13 (t, 3H, J = 6.8 Hz, CH_3), 2.34 (d, 3H, J = 1.2 Hz, CH_3), 4.03 (m, 2H, OCH_2), 6.28 (d, 1H, J = 1.2 Hz, $\text{CH}_{\text{coumarin}}$), 6.45 (s, 1H, CH_{furan}), 7.52 (s, 1H, $1\text{CH}_{\text{aromatic}}$), 7.64 (m, 2H, $2\text{CH}_{\text{aromatic}}$), 7.67 (d, 2H, J = 8 Hz, $2\text{CH}_{\text{aromatic}}$), 8.05 (dd, 1H, J = 8, 1.6 Hz, $1\text{CH}_{\text{aromatic}}$), 8.39 (s, 1H, $1\text{CH}_{\text{aromatic}}$), 12.16 (s, 1H, N–H) ppm; ^{13}C NMR (100.6 MHz, DMSO): δ = 14.4, 18.4, 59.8, 60.4, 109.4, 112.2, 113.9, 117.2, 118.0, 123.7, 123.9, 126.4, 130.5, 134.3, 139.3, 139.5, 148.0, 153.3, 153.6, 160.1, 162.1, 164.8 ppm. MS (EI, 70 eV) (%) 450 (M^+ , 96), 404 (32), 378 (11), 308 (26), 248 (28), 232 (22), 202 (100), 173 (59); anal. calcd. for $\text{C}_{23}\text{H}_{18}\text{N}_2\text{O}_8$ (450.11): C, 61.33; H, 4.03; N, 6.22%; found: C, 61.32; H, 4.01; N, 6.24%.

Methyl 4-(4-methyl-2-oxo-2H-chromen-7-ylamino)-2-(4-bromophenyl)-2,5-dihydro-5-oxofuran-3-carboxylate (4g): Light yellow powder, m.p.: 220–222 °C; IR (KBr): ν_{\max} = 3431, 3060, 2986, 1725, 1648, 1613, 1437 cm^{-1} ; ^1H NMR (400.13 MHz, DMSO): δ = 2.35 (s, 3H, CH_3), 3.61 (s, 3H, OCH_3), 6.23 (s, 1H, $\text{CH}_{\text{coumarin}}$), 6.29 (s, 1H, CH_{furan}), 7.33 (d, 2H, J = 7.6 Hz, $2\text{CH}_{\text{aromatic}}$), 7.43 (d, 2H, J = 7.6 Hz, $2\text{CH}_{\text{aromatic}}$), 7.61 (d, 1H, J = 8.4 Hz, $1\text{CH}_{\text{aromatic}}$), 7.67 (d, 1H, J = 8.4 Hz, $1\text{CH}_{\text{aromatic}}$), 7.72 (s, 1H, $1\text{CH}_{\text{aromatic}}$), 12.04 (s, 1H, N–H) ppm; ^{13}C NMR (100.6 MHz, DMSO): δ = 18.4, 51.7, 60.0, 109.4, 112.5, 113.9, 117.1, 118.0, 121.7, 126.2, 130.5, 131.8, 136.3, 139.5, 152.7, 153.3, 153.6, 160.1, 162.7, 164.8 ppm. MS (EI, 70 eV) (%) 471 (M^+ , 100), 437 (20), 411 (9), 343 (40), 267 (29), 202 (47), 157 (5); anal. calcd. for $\text{C}_{22}\text{H}_{16}\text{N}_2\text{O}_8$ (471.01): C, 56.19; H, 3.43; N, 2.98%; found: C, 56.17; H, 3.42; N, 2.99%.

Methyl 4-(4-methyl-2-oxo-2H-chromen-7-ylamino)-2-(4-chlorophenyl)-2,5-dihydro-5-oxofuran-3-carboxylate (4h): Light yellow powder, m.p.: 265–266 °C; IR (KBr): ν_{\max} = 3434, 2954, 1724, 1656, 1614, 1427 cm^{-1} ; ^1H NMR (400.13 MHz, DMSO): δ = 2.35 (d, 3H, J = 0.8 Hz, CH_3), 3.60 (s, 3H, OCH_3), 6.23 (s, 1H, CH_{furan}), 6.29 (d, 1H, J = 0.8 Hz, $\text{CH}_{\text{coumarin}}$), 7.29 (d, 2H, J = 8.4 Hz, $2\text{CH}_{\text{aromatic}}$), 7.39 (d, 2H, J = 8.4 Hz, $2\text{CH}_{\text{aromatic}}$), 7.61 (dd, 1H, J = 8.8, 2 Hz, $1\text{CH}_{\text{aromatic}}$), 7.67 (d, 1H, J = 8.8 Hz, $1\text{CH}_{\text{aromatic}}$), 7.72 (d, 1H, J = 2 Hz, $1\text{CH}_{\text{aromatic}}$), 11.82 (s, 1H, N–H) ppm; ^{13}C NMR (100.6 MHz, DMSO): δ = 18.4,

51.6, 60.0, 109.4, 112.0, 113.9, 117.0, 118.0, 126.2, 128.9, 130.1, 133.0, 136.1, 139.6, 153.3, 153.4, 153.6, 160.1, 162.9, 165.1 ppm. MS (EI, 70 eV) (%) 425 (M^+ , 100), 393 (19), 366 (9), 297 (14), 223 (46), 202 (48), 155 (18); anal. calcd. for $C_{22}H_{16}ClNO_6$ (425.07): C, 62.05; H, 3.79; N, 3.29%; found: C, 62.03; H, 3.78; N, 3.26%.

Methyl 4-(4-methyl-2-oxo-2H-chromen-7-ylamino)-2,5-dihydro-2-(4-nitrophenyl)-5-oxofuran-3-carboxylate (4i): Light yellow powder, m.p.: 227 °C; IR (KBr): $\nu_{max} = 3437, 3076, 2954, 1728, 1658, 1613, 1522, 1434, 1354 \text{ cm}^{-1}$; $^1\text{H NMR}$ (400.13 MHz, DMSO): $\delta = 2.51$ (s, 3H, CH_3), 3.60 (s, 3H, OCH_3), 6.30 (d, 1H, $J = 0.8$ Hz, $\text{CH}_{\text{coumarin}}$), 6.42 (s, 1H, CH_{furan}), 7.63–7.75 (m, 5H, $5\text{CH}_{\text{aromatic}}$), 8.09 (d, 2H, $J = 8.4$ Hz, $2\text{CH}_{\text{aromatic}}$), 12.26 (s, 1H, N–H) ppm; $^{13}\text{C NMR}$ (100.6 MHz, DMSO): $\delta = 18.4, 51.7, 59.8, 109.4, 111.6, 114.0, 117.2, 118.0, 124.0, 126.4, 129.7, 139.4, 144.9, 147.4, 147.7, 153.3, 153.6, 160.1, 162.8, 165.0$ ppm. MS (EI, 70 eV) (%) 436 (M^+ , 88), 404 (36), 308 (22), 201 (100), 175 (59), 158 (26), 59 (28); anal. calcd. for $C_{22}H_{16}N_2O_8$ (436.09): C, 60.55; H, 3.70; N, 6.42%; found: C, 60.53; H, 3.69; N, 6.44%.

Ethyl 4-(4-methyl-2-oxo-2H-chromen-7-ylamino)-2,5-dihydro-2-(4-nitrophenyl)-5-oxofuran-3-carboxylate (4j): Light yellow powder, m.p.: 201–203 °C; IR (KBr): $\nu_{max} = 3427, 3113, 2980, 1728, 1660, 1613, 1522, 1434, 1355 \text{ cm}^{-1}$; $^1\text{H NMR}$ (400.13 MHz, DMSO): $\delta = 1.13$ (t, 3H, $J = 7.2$ Hz, CH_3), 2.34 (d, 3H, $J = 1.2$ Hz, CH_3), 4.03 (m, 2H, OCH_2), 6.29 (d, 1H, $J = 1.2$ Hz, $\text{CH}_{\text{coumarin}}$), 6.42 (s, 1H, CH_{furan}), 7.64 (dd, 2H, $J = 8.8, 1.6$ Hz, $2\text{CH}_{\text{aromatic}}$), 7.70 (d, 2H, $J = 8.8$ Hz, $2\text{CH}_{\text{aromatic}}$), 7.75 (d, 1H, $J = 1.6$ Hz, $1\text{CH}_{\text{aromatic}}$), 8.09 (d, 2H, $J = 8.8$ Hz, $2\text{CH}_{\text{aromatic}}$), 12.15 (s, 1H, N–H) ppm; $^{13}\text{C NMR}$ (100.6 MHz, DMSO): $\delta = 14.5, 18.4, 59.9, 60.4, 109.3, 112.0, 114.0, 117.2, 117.9, 123.9, 126.4, 129.8, 139.4, 144.9, 147.7, 153.3, 153.5, 153.6, 160.1, 162.2, 164.9$ ppm. MS (EI, 70 eV) (%) 450 (M^+ , 100), 404 (27), 378 (18), 308 (5), 248 (5), 202 (21), 175 (9), 151 (10); anal. calcd. for $C_{23}H_{18}N_2O_8$ (450.11): C, 61.33; H, 4.03; N, 6.22%; found: C, 61.30; H, 4.00; N, 6.25%.

Results and discussion

Characterization of the prepared Fe_3O_4 -PYCA and SA-PYCA- Fe_3O_4 nanoparticles

X-ray diffraction (XRD) analysis

X-ray diffraction using a Cu K_α irradiation was used to characterize the preservation of the crystal structure of the samples after the functionalization step. The result shown in Fig. 1 was fitted for observed six peaks with the following miller indices: (2 2 0), (3 1 1), (4 0 0), (4 2 2), (5 1 1) and (4 4 0) that existing phases were identified as Fe_3O_4 nanoparticles. The average particle diameter was determined by the Scherrer equation [27, 28]. The calculation led for PYCA- Fe_3O_4 to particle sizes

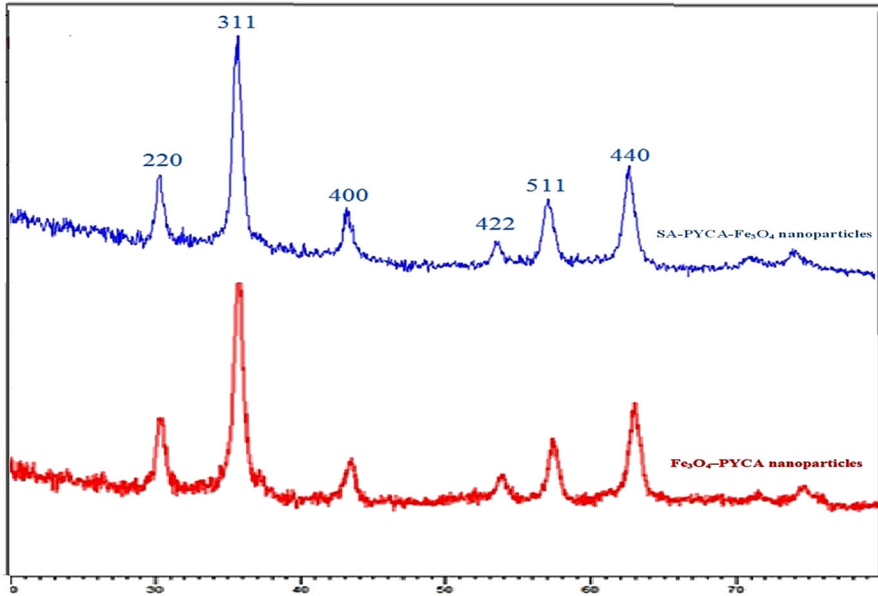


Fig. 1 XRD powder patterns of PYCA-Fe₃O₄ nanoparticles and SA-PYCA-Fe₃O₄ nanoparticles

of about 15 nm and SA-PYCA-Fe₃O₄ nanoparticles sizes of about 21 nm which is in a good agreement with TEM observations.

Fourier transform infrared (FT-IR) analysis

FT-IR measurements were carried out to identify the organic group for capping and efficient stabilization of the synthesized Fe₃O₄ nanoparticles. The FT-IR spectra of Fe₃O₄ appear at 632 and 590 cm⁻¹, which can be ascribed to the vibrations of the Fe–O group. The specific absorption peaks of 1624, 2924 and 2854 cm⁻¹ are attributed to the C=O, C–O and C–H stretching of the PYCA unit, respectively. Reaction of PYCA-Fe₃O₄ with chlorosulfuric acid produces SA-PYCA-Fe₃O₄ in which the presence of a sulfonyl moiety is asserted with 1204 and 1128 cm⁻¹ bands in the FT-IR spectra. Therefore, the data obtained from FT-IR spectroscopy can be confirmed the existence of the nanomagnetic particle and organic group moiety in the structure of SA-PYCA-Fe₃O₄ nanoparticles (Fig. 2).

Thermogravimetric analysis (TGA)

Information about loading of Fe₃O₄ nanoparticles with an organic group was obtained by TGA. The results revealed that the SA-PYCA-Fe₃O₄ nanoparticles contain about 13% of organic material (volatile components disappearing until a temperature of about 100 °C were neglected; Fig. 3). The weight loss of PYCA-modified MNPs appears to be about 6.2% at 300 °C which contributes to the thermal decomposition of the pyridine-4-carboxylic groups. For SA-PYCA-Fe₃O₄,

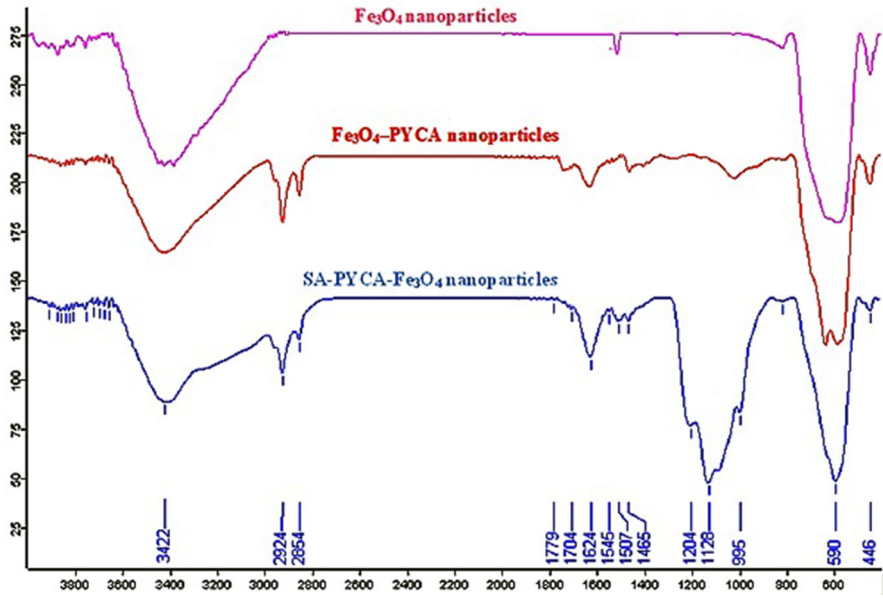


Fig. 2 FT-IR spectra for Fe_3O_4 nanoparticles, PYCA- Fe_3O_4 and SA-PYCA- Fe_3O_4 nanoparticles

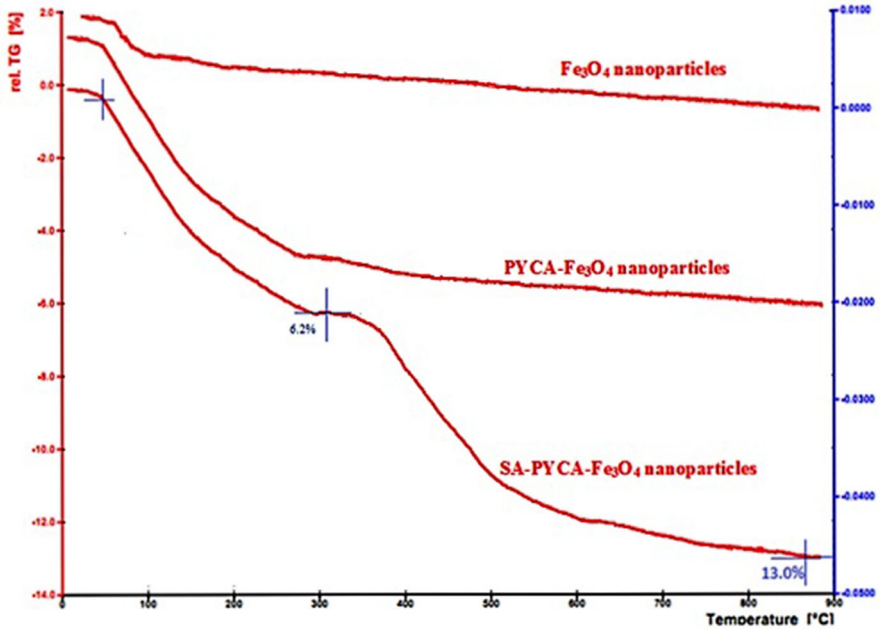


Fig. 3 TGA thermograms of Fe_3O_4 nanoparticles, PYCA- Fe_3O_4 and SA-PYCA- Fe_3O_4 nanoparticles

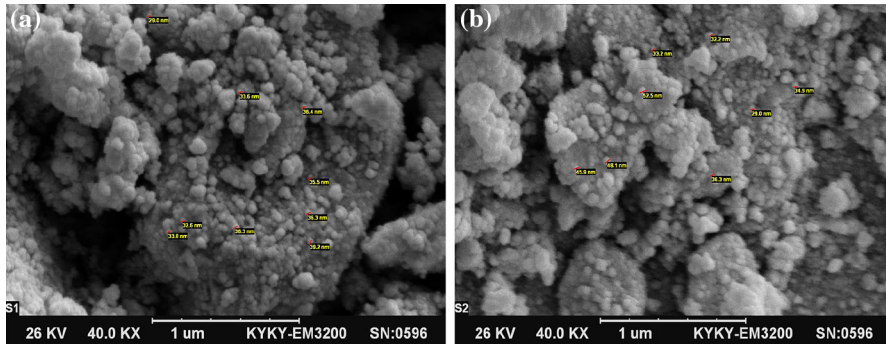


Fig. 4 SEM images of **a** Fe_3O_4 -PYCA and **b** SA-PYCA- Fe_3O_4 nanoparticles

there is a well-defined mass weight loss of 6.8% between 300 and 860 °C related to the breakdown of the SA moieties. On the basis of these results, the good grafting of PYCA and SA groups on the Fe_3O_4 nanoparticles is confirmed.

Scanning electron microscopy (SEM)

The morphological features and size details of synthesized PYCA- Fe_3O_4 nanoparticles and SA-PYCA- Fe_3O_4 nanoparticles were studied by SEM (Fig. 4). The SEM image shows that Fe_3O_4 -PYCA nanoparticles have a mean diameter of about 35 nm. Fig. 4a, b shows SA-PYCA- Fe_3O_4 nanoparticles greater than 43 nm in size. Comparison of experimental results showed the good grafting of PYCA and SA groups on the Fe_3O_4 nanoparticles is confirmed.

Transmission electron microscopy (TEM)

The morphologies of the PYCA- Fe_3O_4 nanoparticles and SA-PYCA- Fe_3O_4 nanoparticles were investigated by TEM (Fig. 5). As can be seen from the TEM images, the average particle size distribution increases from 14 nm in PYCA- Fe_3O_4 nanoparticles

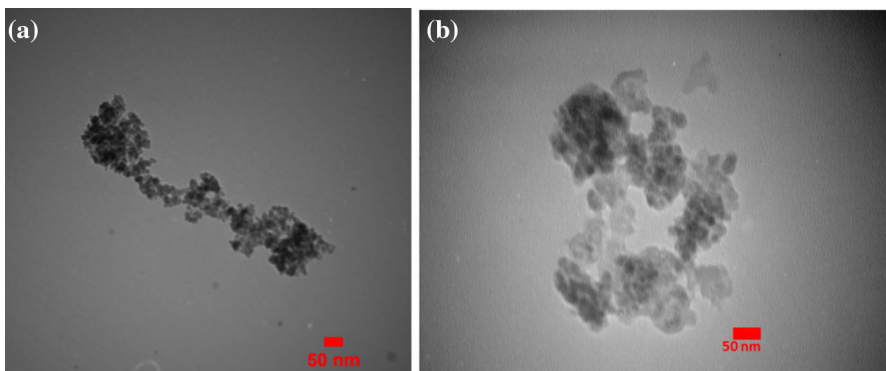


Fig. 5 The TEM images of **a** Fe_3O_4 -PYCA and **b** SA-PYCA- Fe_3O_4 nanoparticles

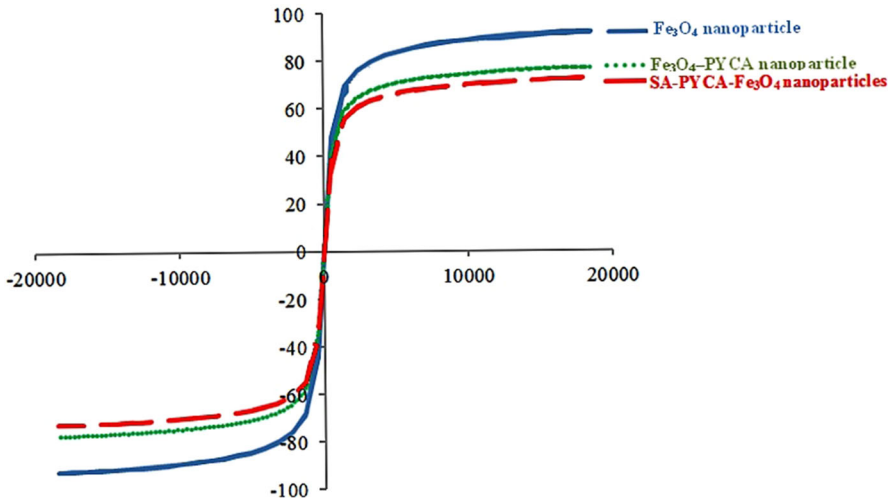


Fig. 6 Room temperature magnetization curves of Fe_3O_4 , Fe_3O_4 -PYCA and SA-PYCA- Fe_3O_4 nanoparticles

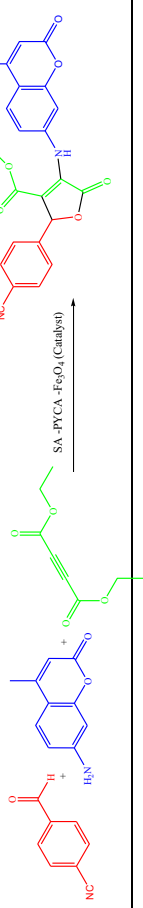
to 19 nm in SA-PYCA- Fe_3O_4 nanoparticles, which is in very good agreement with the crystallite size estimated from XRD. Comparison of experimental results showed the good grafting of PYCA and SA groups on the Fe_3O_4 nanoparticles is confirmed.

Vibrating sample magnetometer (VSM)

Information about magnetic properties of Fe_3O_4 nanoparticles with an organic group supported on Fe_3O_4 nanoparticles was obtained by VSM (Fig. 6). The saturation magnetization values of MNPs, Fe_3O_4 -PYCA nanoparticles and SA-PYCA- Fe_3O_4 nanoparticles were 91.69 emu/g, 73.39 emu/g and 71.20 emu/g, respectively. These differences were caused by the different coating layers and their thicknesses on the surface of Fe_3O_4 nanoparticles. The resulting high values of saturation magnetization of SA-PYCA- Fe_3O_4 nanoparticles enables them to be easily separated and recycled from the products by their response to an external magnetic field.

Catalytic application of SA-PYCA- Fe_3O_4 nanoparticles

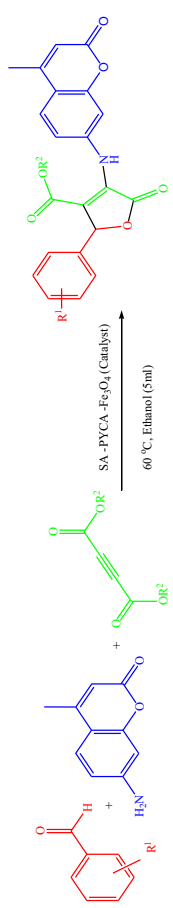
First, to find optimization conditions, the one-pot reaction of 4-cyanobenzaldehyde, 7-amino-4-methylcoumarin and diethyl acetylenedicarboxylate in the presence of the SA-PYCA- Fe_3O_4 as catalyst was selected as a model. The reaction was carried out with different amounts of SA-PYCA- Fe_3O_4 as catalyst (5, 10, 15, 20 mg) in different temperatures (25, 60 °C). The obtained results in Table 1 show that optimal condition was 15 mg of SA-MNPs at 60 °C (Table 1, entry 4).

Table 1 Optimization conditions for preparation of compound **4d** in the presence of different amount of SA-PYCA-Fe₃O₄ as catalyst in different temperatures


Entry	Amount of catalyst (mg)	Temperature (°C)	Time (h)	Yield (%) ^a
1	Free catalyst	25	10	–
2	Free catalyst	60	10	–
3	Free catalyst	Reflux	10	–
4	5	25	10	Trace
5	10	25	10	37
6	15	25	8	48
7	20	25	7	54
8	5	60	5	50
9	10	60	4	80
10	15	60	2.5	93
11	20	60	2.5	94
12	5	Reflux	3	70
13	10	Reflux	2.5	85
14	15	Reflux	2.5	95
15	20	Reflux	2.5	96

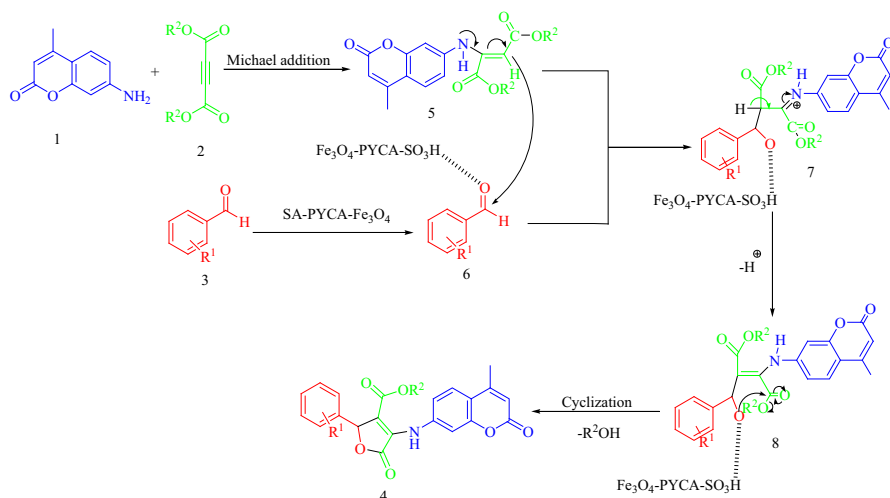
^a Yields refer to isolated pure product

Table 2 Multi-component synthesis of *N*-coumarin-2-furanone derivatives using aromatic aldehydes, 7-amino-4-methylcoumarin and dialkyl acetylenedicarboxylate in the presence of SA-PYCA-Fe₃O₄ as catalyst



Entry	Compounds	R ¹	R ²	Time (h)	Yields of compound 4a-j (%) ^a	Melting point (°C)
1	4a	H	OCH ₃	2.5	75	220
2	4b	H	OCH ₂ CH ₃	3	72	250–251
3	4c	4-CN	OCH ₃	2	92	200–202
4	4d	4-CN	OCH ₂ CH ₃	2	91	255–256
5	4e	3-NO ₂	OCH ₃	2.5	88	285–286
6	4f	3-NO ₂	OCH ₂ CH ₃	2.5	87	270–271
7	4g	4-Br	OCH ₃	2	90	220–222
8	4h	4-Cl	OCH ₃	2	92	265–266
9	4i	4-NO ₂	OCH ₃	2	91	227
10	4j	4-NO ₂	OCH ₂ CH ₃	2	88	201–203
11	4k	4-OCH ₃	OCH ₃	24	–	–
12	4l	4-OH	OCH ₃	24	–	–
13	4m	4-CH ₃	OCH ₃	24	–	–
14	4n	2-OCH ₃	OCH ₃	24	–	–
15	4o	2-OH	OCH ₃	24	–	–
16	4p	4-CH ₃	OCH ₂ CH ₃	24	–	–
17	4q	Butyraldehyde	OCH ₃	24	–	–
18	4r	Butyraldehyde	OCH ₂ CH ₃	24	–	–

^a Yields refer to the isolated pure products



Scheme 4 Suggested mechanism for the synthesis of *N*-coumarin-2-furanones derivatives in the presences of SA-PYCA-Fe₃O₄ nanocatalyst

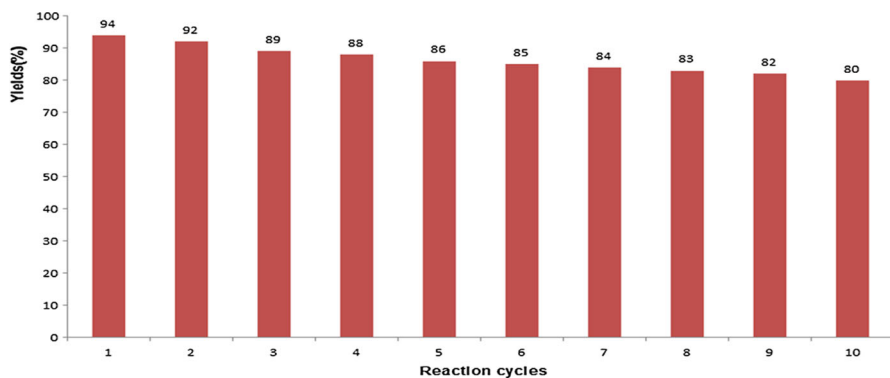


Fig. 7 Recycling of the SA-PYCA-Fe₃O₄ as catalyst

Next, the reactions were performed with various aromatic aldehydes including electron-donating groups and electron-withdrawing substituents in the presence of SA-PYCA-Fe₃O₄ catalyst. As shown in Table 2, aldehyde-containing electron-withdrawing groups such as NO₂, CN, Cl and Br (entries 3–10) led to the corresponding products in high yields, but the aldehyde-containing electron-donating groups such as CH₃, OCH₃ and OH (entries 11–16) did not afford the desired products.

The structure of **4d** was confirmed by FT-IR, ¹H NMR, ¹³C NMR and mass spectra, as well as elemental analysis. The FT-IR spectrum of **4d** showed a broad band at 3421 cm⁻¹ for the N–H stretching, a medium signal at 2231 cm⁻¹ for the nitrile group and two peaks at 1724 and 1648 cm⁻¹ for the two C=O groups of the ester and amide moieties, respectively. The ¹H NMR spectrum of **4d** exhibited a



Fig. 8 Image showing SA-PYCA-Fe₃O₄ nanoparticles can be separated by an applied magnetic field. A reaction mixture in the absence (*right*) or presence of a magnetic field (*left*)

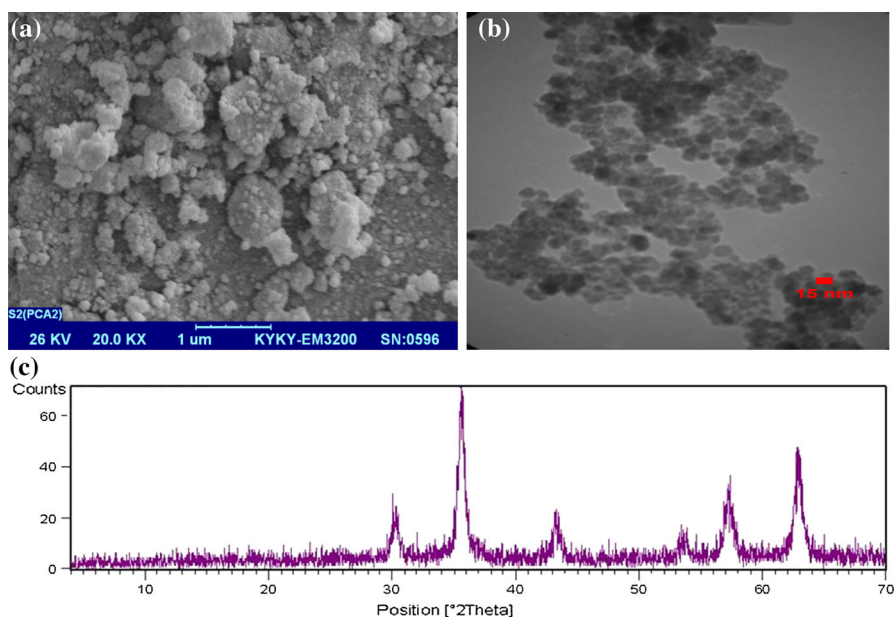


Fig. 9 a SEM, b TEM and c XRD analysis of SA-PYCA-Fe₃O₄ nanoparticles after recycling four times

triplet at $\delta = 1.24$ ppm (${}^3J_{HH} = 7.2$ Hz) for the methyl group, a doublet at $\delta = 2.38$ ppm (${}^4J_{HH} = 1.2$ Hz) for the methyl group of coumarin, a quartet 4.25 ppm (${}^3J_{HH} = 7.2$ Hz) for the OCH₂, a singlet at $\delta = 5.85$ ppm for the CH group of furan-2(5*H*)-one moiety, a doublet at $\delta = 6.23$ ppm (${}^4J_{HH} = 8.8$ Hz) for the =CH groups of coumarin and two doublets at $\delta = 7.42$ and 7.61 ppm (${}^3J_{HH} = 8.4$ Hz) for the four CH groups of the para-substituted benzene ring and two doublets at $\delta = 7.36$ (${}^4J_{HH} = 2.4$ Hz) and 7.53 (${}^3J_{HH} = 8.8$ Hz) as well as a doublet of a doublet at $\delta = 7.71$ ppm (${}^3J_{HH} = 8.8$ Hz, ${}^4J_{HH} = 2$ Hz) for the three

protons of the phenyl group of coumarin. The NH group appeared at $\delta = 9.14$ ppm as a broad signal. The ^{13}C NMR spectrum of **4a** exhibited 22 signals in agreement with the proposed structure. The mass spectrum of this compound displayed a molecular ion peak at m/z 430 (M^+) and the other fragments at 384, 357, 201, 155 and 127 in accordance with the structure of **4d**.

A proposed mechanism for the reaction was shown in Scheme 2. First, the enamine **5** was formed from the reaction of 7-amino-4-methylcoumarin **1** and dialkyl acetylenedicarboxylate **2**. Then, enamine **5** attacked to the activated aromatic aldehyde **6** that protonated with SA-PYCA- Fe_3O_4 as acidic catalyst. The intermediate **7** is converted to intermediate **8** by loss of a proton. Finally, compound **8** perform a cyclization reaction with loss of ROH to produce compound **4** (Scheme 4).

We also investigated the recycling of the SA-PYCA- Fe_3O_4 as the catalyst using the model reaction of 4-cyanobenzaldehyde, 7-amino-4-methylcoumarin and diethyl acetylenedicarboxylate in ethanol (5 mL; Table 2, entry 4). When the reaction was complete, the reaction mixture was cooled to ambient temperature and solvent was removed on a rotary evaporator. Then, the mixture was diluted with CH_2Cl_2 and the SA-PYCA- Fe_3O_4 nanoparticles were separated by magnetic field for separation of the catalyst, and the reusability under similar reaction conditions was checked. The results showed that SA-PYCA- Fe_3O_4 is a stable catalyst in reaction media and can be reused ten times without significant loss of its catalytic activity (Figs. 7, 8). The SEM, TEM and XRD analysis of recycled SA-PYCA- Fe_3O_4 was provided and shown in Fig. 9.

Conclusions

In this research, we described synthesis, characterization and catalytic applications of novel SA-PYCA- Fe_3O_4 MNPs for preparation of novel *N*-coumarin-2-furanones derivatives from arylaldehydes, 7-amino-4-methylcoumarin and dialkyl acetylenedicarboxylate. The attractive features of this procedure are a simple procedure, cleaner reaction and use of a nanocatalyst with good reversibility.

Acknowledgements This research was supported by the Research Council of the University of Mazandaran in Iran.

References

1. A. Tiwari, A.K. Mishra, H. Kobayashi, A.P.F. Turner, *Intelligent Nanomaterials* (Wiley, New Jersey, 2012)
2. C.N.R. Rao, A. Müller, A.K. Cheetham, *The Chemistry of Nanomaterials: Synthesis, Properties and Applications*, vol. 1 (Wiley, Weinheim, 2006)
3. K.J. Klabunde, R. Mulukutla, *Nanoscale Materials in Chemistry* (Wiley, New York, 2001)
4. A. Wang, X. Liu, Z. Su, H. Jing, *Catal. Sci. Tech.* **4**, 71–80 (2014)
5. S. Fan, W. Dong, X. Huang, H. Gao, J. Wang, Z. Jin, J. Tang, G. Wang, *ACS Catal.* **7**, 243–249 (2016)
6. K. Mishra, T.N. Poudel, N. Basavegowda, Y.R. Lee, *J. Catal.* **344**, 273–285 (2016)
7. H.N. Dadhania, K.R. Dipak, N.D. Abhishek, *Catal. Sci. Tech.* **5**, 4806–4812 (2015)

8. X. An, D. Cheng, L. Dai, B. Wang, H.J. Ocampo, J. Nasrallah, X. Jia, J. Zou, Y. Long, Y. Ni, *Appl. Catal. B* **206**, 53–64 (2017)
9. K. He, Y. Ma, B. Yang, C. Liang, X. Chen, C. Cai, *Spectrochim. Acta Mol. Biomol. Spectrosc.* **173**, 82–86 (2017)
10. S. Liu, H. Wang, L. Chai, M. Li, *J. Colloid Interface Sci.* **478**, 288–295 (2016)
11. R. Mirzajani, S. Ahmadi, *J. Ind. Eng. Chem.* **23**, 171–178 (2015)
12. M.A. Rahman, U. Culsum, A. Kumar, H. Gao, N. Hu, *Int. J. Biol. Macromol.* **87**, 488–497 (2016)
13. C.M. Volla, I. Atodiresei, M. Rueping, *Chem. Rev.* **114**, 2390–2431 (2013)
14. A. DeAngelis, M.T. Taylor, J.M. Fox, *J. Am. Chem. Soc.* **131**, 1101–1105 (2009)
15. J. Sun, E.Y. Xia, Q. Wu, C.G. Yan, *Org. Lett.* **12**, 3678–3681 (2010)
16. H. Dong, L. Xu, S.S. Li, L. Wang, C.L. Shao, J. Xiao, *ACS. Comb. Sci.* **18**, 604–610 (2016)
17. S. Mirza, S.A. Naqvi, K.M. Khan, U. Salar, M.I. Choudhary, *Bioorg. Chem.* **70**, 133–143 (2017)
18. M.R.M. Shafiee, S.S. Mansoor, M. Ghashang, A. Fazlinia, *C. R. Chim.* **17**, 131–134 (2014)
19. L. Nagarapu, U.N. Kumar, P. Upendra, R. Bantu, *Synth. Commun.* **42**, 2139–2148 (2012)
20. A. Kathuria, N. Priya, K. Chand, P. Singh, A. Gupta, S. Jalal, S. Gupta, H.G. Raj, S.K. Sharma, *Bioorg. Med. Chem.* **20**, 1624–1638 (2012)
21. M. Mazzei, E. Nieddu, M. Miele, A. Balbi, M. Ferrone, M. Fermeglia, M.T. Mazzei, S. Pricl, P. La Colla, F. Marongiu, C. Ibba, *Bioorg. Med. Chem.* **16**, 2591–2605 (2008)
22. A.M. Hamdy, Z. Khaddour, N.A. Al-Masoudi, Q. Rahman, C. Hering-Junghans, A. Villinger, P. Langer, *Bioorg. Med. Chem.* **24**, 5115–5126 (2016)
23. M. Bozdog, A.M. Alafeefy, A.M. Altamimi, D. Vullo, F. Carta, C.T. Supuran, *Bioorg. Med. Chem.* **25**, 677–683 (2017)
24. A. Montagut-Romans, M. Boulven, M. Jacolot, S. Moebs-Sanchez, C. Hascoët, A. Hamed, S. Besse, M. Lemaire, E. Benoit, V. Lattard, F. Popowycz, *Bioorg. Med. Chem. Lett.* **27**, 1598–1601 (2017)
25. S. Asghari, M. Mohammadnia, *Res. Chem. Intermed.* **42**, 1899–1911 (2016)
26. S. Asghari, M. Mohammadnia, *Synth. React. Inorg. Met. Org. Chem.* **47**, 1004–1011 (2017)
27. T. Wejrzanowski, R. Pielaszek, A. Opalińska, H. Matysiak, W. Łojkowski, K. Kurzydłowski, *J. Appl. Surf. Sci.* **253**, 204–208 (2006)
28. R. Pielaszek, *J. Appl. Crystallogr.* **1**, 43–50 (2003)